Elastic behaviour characterisation of TRIP 700 steel by means of loading-unloading tests

Joseba Mendiguren[a,1,*], Fernando Cortés[b,1], Xabier Gómez[a,1], Lander Galdos[a,1]

[a] *Mechanical and Industrial Manufacturing department, Mondragon Unibertsitatea, Loramendi 4, 20500 Mondragón, Spain*
[b] *Deusto Institute of Technology (DeustoTech), Faculty of Engineering, University of Deusto, Avda. de las Universidades 24, 48007 Bilbao, Spain*

Abstract

The elastic behaviour of TRIP 700 steel under plastic deformation is analysed. The analysis is carried out by means of classical tensile test and loading-unloading cyclic tests. These tests have been performed using high deformation strain gages, which enable an accurate and continuous measurement of strain.

An elastic modulus reduction of 20% is observed for 12% plastic deformation. Furthermore, non-linear unloading and loading paths have been found in this work. This is an important difference with respect to other authors and opens new possibilities for the development of new material models to improve the prediction of the post forming springback of industrial parts, which is an important issue for the automotive industry.

Keywords: Springback, TRIP 700, Elastic unloading, Non-linear elastic loading, inelasticity, pseudo young modulus.

*Corresponding author
Email address: jmendiguren@mondragon.edu (Joseba Mendiguren)
[1]Tel.: +34 943794700; fax: +34 943791536.

1. Introduction and objective

Fuel consumption diminution and car safety improvement have been the last decade drivers in the automotive industry. In this context, new material families and forming processes have been introduced in workshop, advanced high strength steels (hereafter AHSS) being a clear example. These steels present high yield strength, poor formability and a common problem of subsequent springback after forming.

In the last decade, both experimental techniques and numerical models have improved aimed at representing more accurately the prediction of springback. As example Cleveland and Ghosh experimentally analysed both the hardening and the inelastic behaviours of the GP50XK60 high strength steel concluding the importance of an accurate material modelling for a correct stamping simulations. Eggertsen and Mattiasson on the other hand, studied the influence of the yield criteria and hardening model selection on the springback prediction of an U-channel test. They showed that not only the model selection but the characterization method as well were found to be crucial for an accurate springback prediction.

A widely used AHSS is the TRIP 700 steel, which consists in a ferritic matrix, containing bainite, martensite and a fraction of metastable retained austenite. Under plastic deformation, the transformation induced plasticity (hereafter TRIP) effect is triggered, which signifies that retained austenite is transformed into martensite. This phenomenon induces advantageous me-

chanical properties due to strain hardening making it interesting for critical structural body parts.

When a TRIP steel is plastically deformed, Morestin and Boivin (1996) found that elastic modulus decreases more than 10% with only 5% of plastic strain. Perez et al. (2005) and more recently Yu (2009) and Mendiguren et al. (2012) performed elastic unloading characterisation of different TRIP steels by means of loading-unloading cyclic tests.

Due to the important impact that elastic modulus reduction has on springback simulations, different authors have implemented this variation into finite element codes improving the springback prediction accuracy. Gelin et al. introduced the elastic modulus degradation of a TRIP steel function of the martensite volume fraction on a cylindrical cup drawing process while Fei and Hodgson implemented the reduction of the elastic modulus function of plastic strains for V-bending test modelling. Recently, Sun and Wagoner introduced the concept of a quasi-plastic-elastic strain to explain the non-linear elastic recovery characteristic of the AHSS while Mendiguren et al. made an extension of the classic elastic law using fractional derivatives to be able to represent these non-linear behaviours.

In this work, the elastic behaviour of TRIP 700 steel has been studied, strain being measured more accurately than in previous works by means of large deformation strain gages. This allows continuous measurement of strain during the whole test avoiding the stop of the test at each cycle.

Through this new proposed strain measurement method, some conclusions drown in previous works have been validated, while different data have been obtained on others. The characterization tests have been carried out by means of conventional tensile test and loading-unloading cycles (Mendiguren et al., 2012). The loading-unloading cyclic tests have been performed up to near 20%.

The paper is structured as follows:

- Firstly, the materials and experimental procedures are presented
- Next, the results of a tensile test and the loading-unloading cycles are shown
- Then, the results are discussed analysing the micro-phenomena involved in the macro-elastic behaviour
- Finally, conclusions about the elastic behaviour of the TRIP 700 steel are pointed out

2. Experimental procedure

2.1. Material and specimens

TRIP 700 steel 1.5 mm thickness has been studied in the present work. The chemical composition obtained by optical emission spectroscopy is shown in Table 1.

The testing specimens have been cut from a flat sheet at 0º, 45º and 90º rolling directions following the EN 10 002-1 standard (see Fig. 1). Three

Table 1

Chemical composition (wt%) of the analysed TRIP 700 steel.

C	Si	Mn	P	S	Cr	Ni	Mo	Al	Cu
0.22	0.29	1.82	0.012	0.002	0.03	0.02	0.04	0.86	0.03

specimens for each direction have been produced by means of wire EDM in order to minimise the influence of the cutting process on the microstructure and behaviour of the material.

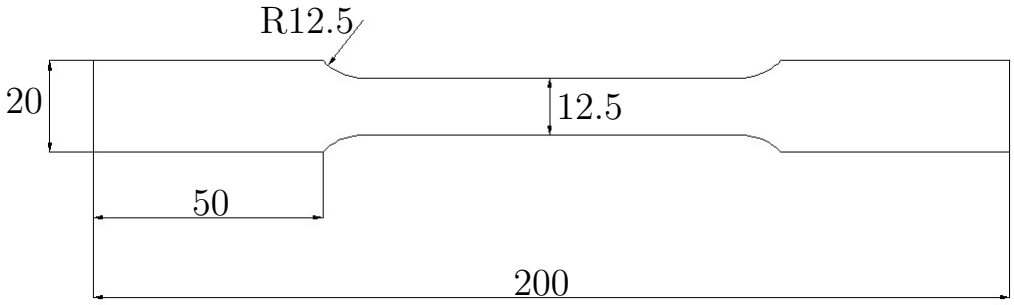

Figure 1: Dimensions (in mm) of the testing specimens following the EN 10 002-1 standard.

A complementary DC04 mild steel material has been used in this study as a lower carbon content comparative material. The chemical composition obtained by optical emission spectroscopy is shown in Table 2.

Table 2

Chemical composition (wt%) of the analysed DC04 mild steel.

C	Si	Mn	P	S	Cr	Ni	Al	Cu
0.06	0.02	0.22	0.15	0.007	0.03	0.02	0.05	0.01

2.2. Experimental technique

In order to obtain an accurate and continuous measurement of the strain, high deformation Vishay-EP-08-250BF-350 strain gages have been used. These special gages are assembled using fully annealed constantan foils with high elongation polyimide backing. A properly bonded and wired gage is able to measure deformations up to 20%. Experimental set-up is shown in Fig.2. Two strain gages can be observed, in the longitudinal direction and the transversal direction. Only the longitudinal one is used in the present work, the latter one being used for a parallel work to characterize the anisotropy coefficients in function of the plastic strain. Additionally, an extensometer has been used for the machine control.

Conventional tensile tests and cyclic tests have been carried out for the elastic behaviour characterisation. The conventional tensile tests have been carried out according to the EN 10 002-1 standard in an Universal 5 t Instron-Zwick/Roell machine. The tests have been performed at 3 mm/min velocity, which gives an approximate strain rate of $1 \times 10^{-3}\,\mathrm{s}^{-1}$.

Using the same machine, cyclic tests have been performed, where the specimen is stretched until a defined specific strain, called hereafter pre-strain $\varepsilon_{\mathrm{ps}}$,

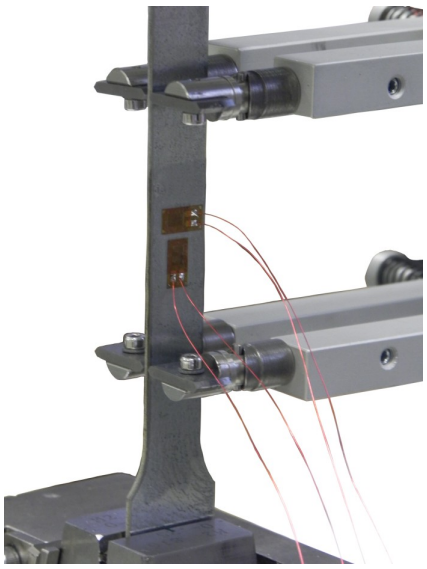

Figure 2: Experimental set up for the different tensile tests.

and then unloaded to the relaxed state (zero stress). Once the first loading-unloading cycle is finished, the specimen is reloaded again until a higher pre-strain and subsequently unloaded. This procedure is repeated several times. The influence of the pre-strain levels have been studied by the authors in a previous work (Mendiguren et al. (2012)) concluding the invariability of the elastic behaviour of the material due to the elastic unloading-loading cycles. Therefore, as the elastic behaviour of the material is not affected by the number of experimental cycles or their pre-strain, non-equispaced pre-strain levels $\varepsilon_{\mathrm{ps}}$ have been selected in this work as shown in Table 3.

Table 3

Pre-strain levels $\varepsilon_{\mathrm{ps}}$ for the loading-unloading cyclic tests.

Cycle	1	2	3	4	5	6	7	8
$\varepsilon_{\mathrm{ps}}$	0.015	0.030	0.045	0.060	0.090	0.120	0.160	0.190

3. Experimental results

3.1. Conventional tensile tests

The flow curves of the TRIP 700 material for the three different rolling directions are shown in Fig. 3. From these data, Young modulus has been obtained by curve fitting following the ASTM-E111-97 standard. The obtained Young modulus is very similar in the three directions. The average value of 204 ± 5.25 GPa is considered in this work as initial modulus .

3.2. Loading-unloading cyclic tests

Figure 4 shows the mean flow curve of the 0º specimens after loading-unloading cyclic test, the conclusions derived from the analysis of the other two directions being equivalent. The maximum strain is 18.5%, because no gage resisted a higher deformation.

By comparing this curve with the 0º curve of Fig. 3, it can be concluded that the global mechanical behaviour of the material remains the same and hardening is not affected by the cyclic loads (less than 1.5% difference between the conventional and cyclic flow curve). However, from Fig. 4 two

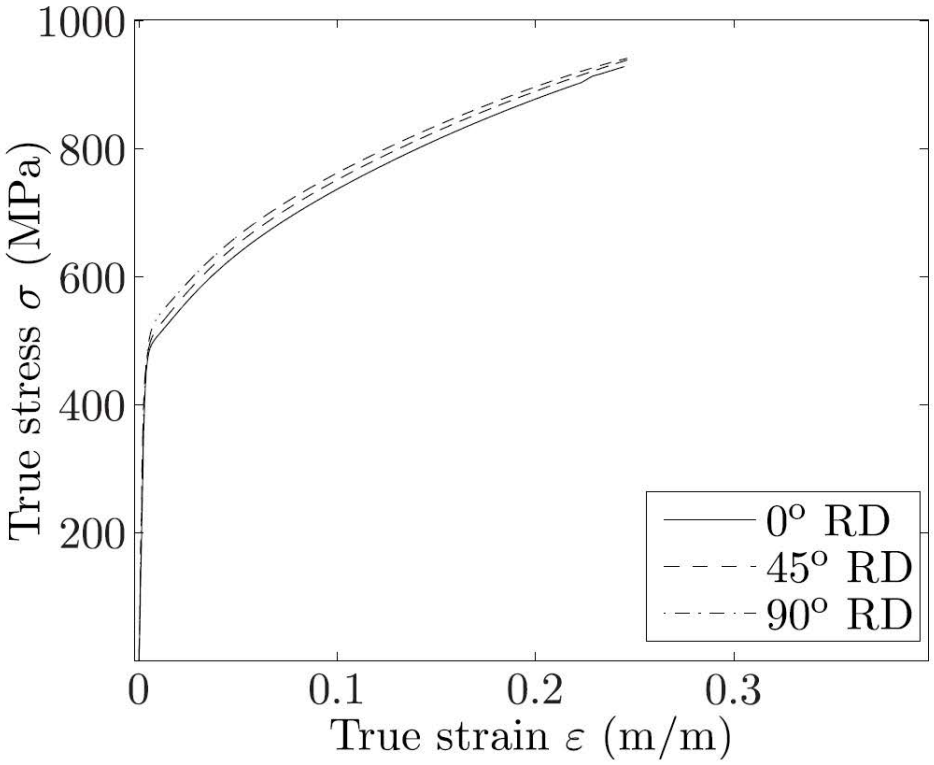

Figure 3: True stress-true strain curves for the three rolling directions.

particularities can be drawn. On the one hand, the upper yield point increases every loading-unloading cycle. On the other hand, it can be observed that the slope of the loading-unloading paths diminishes as strain is higher. Besides, by means of a thorough comparison between an unloading path and its corresponding loading one, it can be concluded that both paths are non-linear and slightly different, originating a tight loop.

In order to deeply analyse the elastic behaviour of this material, the curves

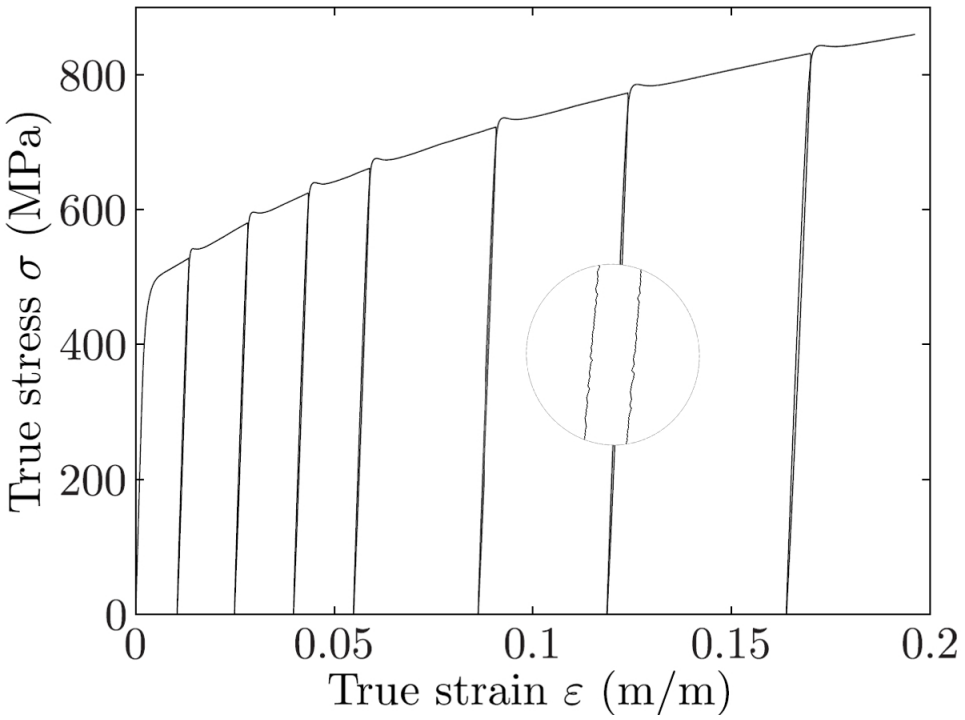

Figure 4: True stress-true strain curve for 0^o specimens loading-unloading cyclic test.

are minutely analysed next. Four different studies are carried out:

- The evolution of the elastic modulus in loading paths
- The non-linear behaviour of loading paths
- The evolution of the elastic modulus for unloading paths
- The non-linear behaviour of unloading paths

3.2.1. Evolution of the elastic modulus in loading paths

In this section each loading phase has been assumed to be linear. In this context, the elastic modulus has been obtained according to the same strategy followed for calculation of the Young modulus. At this point, it is important to highlight that in this paper Young modulus is refereed to the slope of the first loading path, when the material is not plastically deformed, whereas for the slope of all other loading paths, it is used the term elastic modulus. Three specimens have been tested for each orientation. The mean value and standard deviation of elastic modulus at each cycle pre-strain is presentd in Fig. 5. The maximum pre-strain is 12%, as only one gage resisted higher strains. From these results it can be concluded that the elastic modulus decreases $15 - 20\%$ with plastic a deformation of 12%.

3.2.2. Non-linear behaviour of loading paths

If the loading phases are meticulously analysed, it can be remarked that they are non-linear. In order to characterise this non-linearity, the instantaneous elastic modulus $\mathrm{d}\sigma/\mathrm{d}\varepsilon$ is computed and represented in Fig. 6, only for the 0^{o} direction. The conclusions derived from the other two directions are very similar.

It can be concluded that the instantaneous elastic modulus decreases from around 200 GPa to 90 GPa as stress grows, which illustrates the assertion of the non-linearity of the loading paths.

3.2.3. Evolution of the elastic modulus for unloading paths

Figure 7 shows a representative unloading phase, the one of the 16% of pre-strain. The unloading stress-strain curve is not a straight line but a curve.

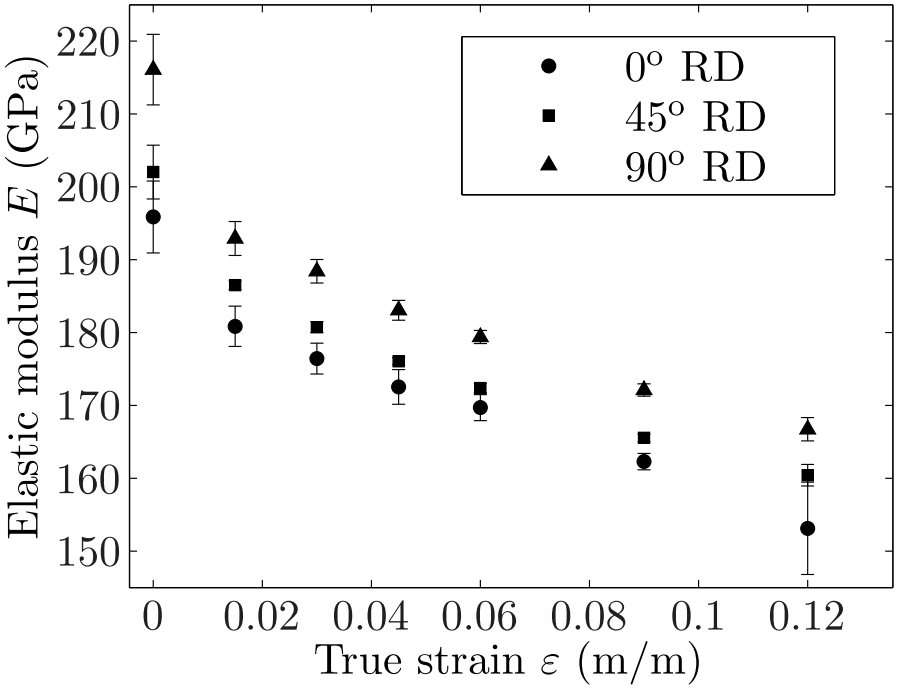

Figure 5: Loading elastic modulus at different pre-strains for the three material directions.

The slope of the straight line that links the first and the last stress-strain points is defined as the chord modulus E_{ch} and it represents a characteristic parameter for springback simulations. As it is shown in Fig. 7, the chord modulus is lower than the Young modulus previously obtained.

From the three specimens tested for each material direction, the average chord modulus is computed and represented in Fig. 8. The chord modulus decreases as the plastic strain grows. In the first unloading cycle, after 1.5% of strain, it is around 180 GPa while after 12% of pre-strain this value decreases down to 150 GPa. This data reveals the importance of such a characterization

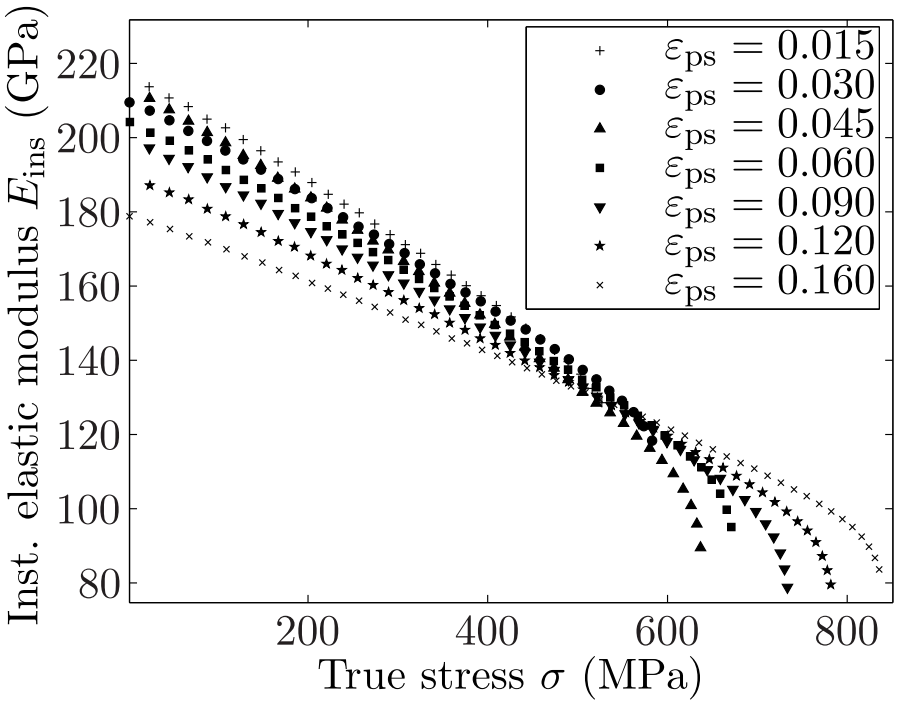

Figure 6: Loading instantaneous elastic modulus for each loading phase. Results from the 0° RD specimen.

for a reliable process simulation.

3.2.4. Non-linear behaviour of unloading paths

As for the loading case, in order to analyse the non-linearity of the elastic unloading, the instantaneous elastic modulus $\mathrm{d}\sigma/\mathrm{d}\varepsilon$ is computed for the 0° direction specimen. The results are shown in Fig. 9. Two conclusions can be obtained. On the one hand, it can be pointed out that the bigger the pre-strain ε_{ps} is the lower the instantaneous elastic modulus becomes. On the other hand, for each unloading phase, the instantaneous elastic modulus decreases as stress goes down. For the seven tested pre-strains, the instan-

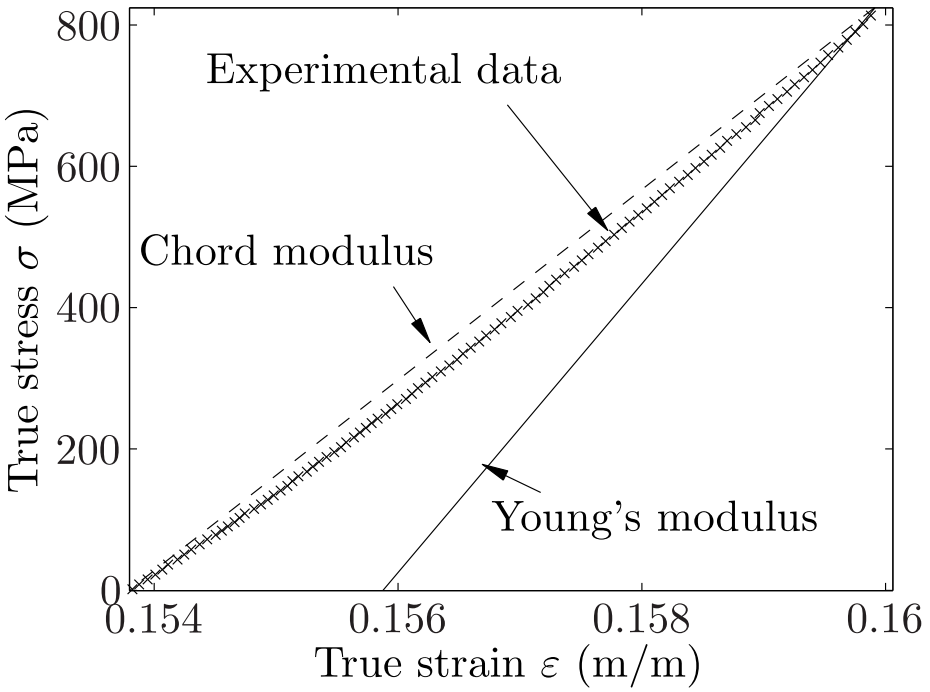

Figure 7: Unloading stress-strain curve obtained by experiment and curves calculated with chord modulus and Young's modulus when strained to 0.16.

taneous elastic modulus decreases with an approximate slope equal to 50 GPa/GPa .

4. Discussion

4.1. About the elastic behaviour

In the present work the reduction of the elastic modulus reaches the $15 - 20\%$ for a 12% of pre-strain.

Yu in 2009 arrived to a similar conclusion for the TRIP 600 steel, measuring a reduction of a 20% for 30% of plastic strain. On the other hand,

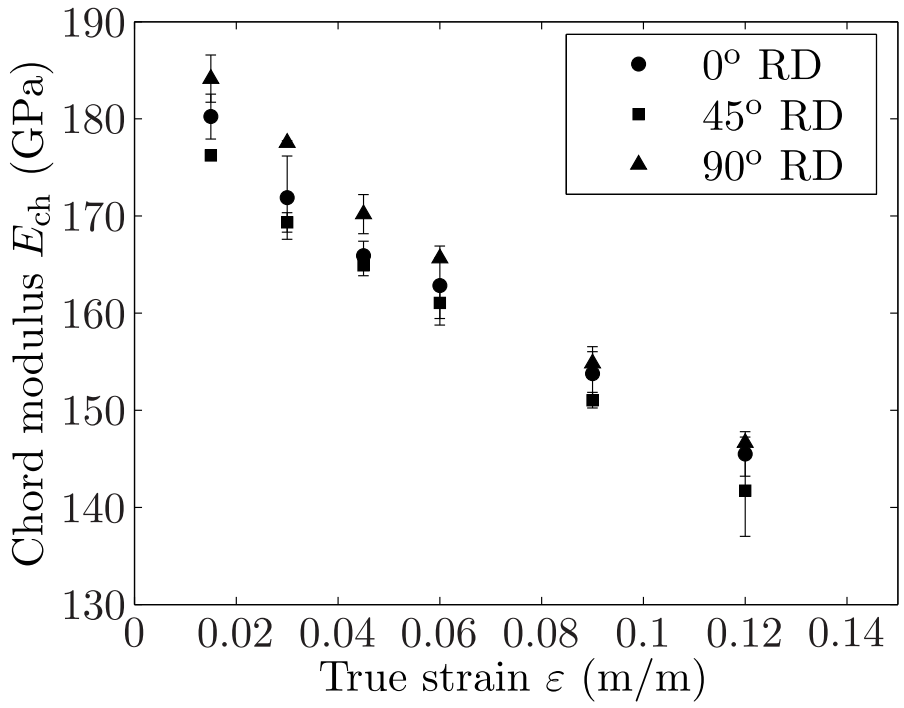

Figure 8: Chord modulus evolution at different pre-strains for three material directions.

Perez et al. in 2005 analysed this phenomenon for the TRIP 700 and they concluded that the elastic modulus for the TRIP 700 diminishes quickly in the first stage of deformation, followed by a slight and constant drop as strain grows, where the final decrease in the elastic modulus at 20% of pre-strain was about $5 - 6\%$.

The disagreement between the results presented by Perez et al. and those presented in this work can be due to the different techniques used to measure the strain. Perez et al. measured the strain with one strain gage at each cycle while in the present work a unique strain gage has been used along all the

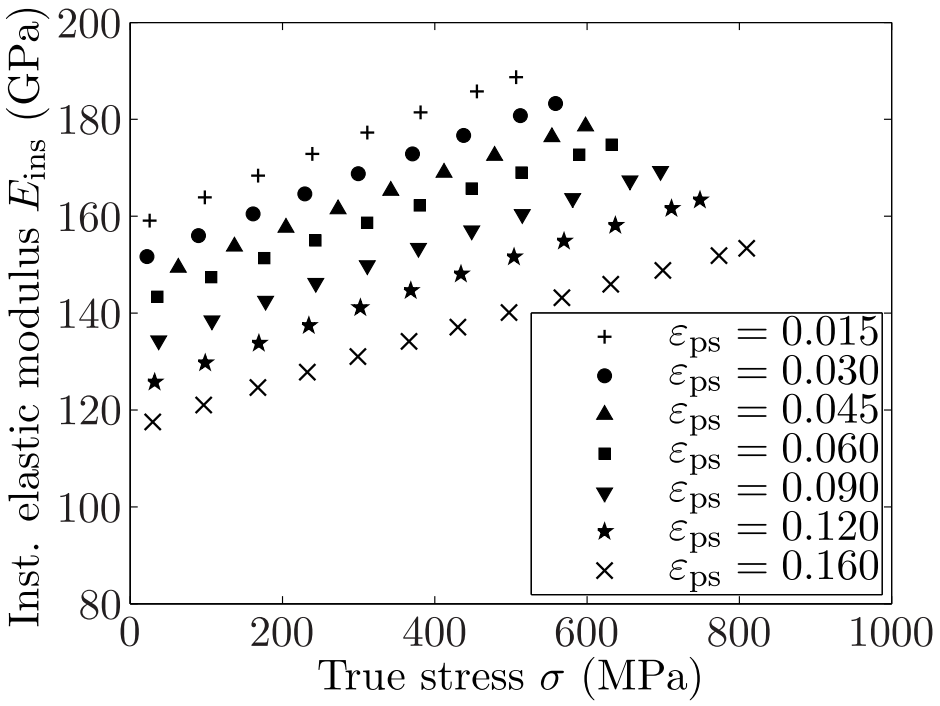

Figure 9: Unloading instantaneous slope for each unloading phase. Results from the 0º RD specimen.

test avoiding in this way the manipulation of the sample during the test.

In the literature two different theories can be found to explain why the elastic modulus decreases with the plastic deformation. On the one hand, the theory relating the elastic modulus diminution with the TRIP effect (i.e. the retained austenite is transformed into martensite as plastic deformation increases), based on the fact that the elastic properties of austenite and martensite are quite different (Doege et al., 2002). In this context, Thibaud et al. (2002) proposed an exponential relationship between the elastic modulus and the martensite volume fraction.

On the other hand, the second theory, Perez et al. (2005), states that elastic modulus reduction is related with the dislocation behaviour instead of the martensite volume fraction. Perez et al. (2005) concluded that during the first part of the deformation process the total amount of transformed austenite is high. The transformation rate decreases as the strain increases reaching an untransformed austenite therefore around $2-3$ %. Consequently, the TRIP effect cannot explain the modulus evolution at higher strains. Due to previous facts, they concluded that the microplastic stains are the the main reason for which the elastic modulus decreases with the pre-strain. Microplastic strains are related with the dislocation movement though the grain and their pile-ups on the grain boundaries, see the original work for more details.

Concerning the non-linearity of the unloading path, it must be mentioned that this phenomenon has been already shown in previous works, Perez et al. analysed this phenomena for some TRIP steels while as previously mentioned Sun and Wagoner and Mendiguren et al. developed a new modelling techniques to represent this unloading path. This non-linear unloading path can be explained in terms of microplastic strain (Perez et al., 2005). During plastic deformation, dislocations move through the grain and at the same time new dislocations are created (Foreman, 1967). Under stress conditions, despite these dislocations are repellent one to another, they form pile-ups into the grain boundaries. When the stress is removed, unloading dislocations tend to adopt a new configuration corresponding to an equilibrium state. The going back of dislocations produces an extra strain resulting in a

non-linear unloading path. Apart from the microplastic strain recovery, the unloading recovery is governed by the classical interatomic plane relocation and the bended dislocations unbending too.

If the loading and the unloading behaviours are compared, two conclusions can be drawn. Even if the unloading and subsequent loading phases do not follow the same path, both of them start and finish approximately at the same point. Therefore, the chord moduli obtained from the unloading and the elastic modulus of the loading phases are very closed to each other.

The second observation is that, around the zero stress state, in the loading phases all the loading instantaneous elastic moduli start between 180 GPa and 220 GPa. However, for the unloading behaviour, each unloading phase reaches the zero stress state with different instantaneous elastic modulus between 120 GPa and 160 GPa. Likewise, around the yield stress in the loading behaviour all the loading phases reaches the range of 140-120 GPa (further than this starts the elastoplastic behaviour).

4.2. About the upper yield point

As it has been previously mentioned, an increase of the upper yield point is shown when the specimen is reloaded after an unloading phase (see Fig. 4). This phenomenon could be explained by the strain ageing process. Strain ageing is divided into three main stages in time. In the first stage, the short time Snoek rearrangement process is activated, which is an effect of the stress-induced rearrangement of the interstitial atoms in the stress field of dislocations (Farías, 2006). The medium time dislocation pinning governed by the Cottrell effect composes the second stage. The last stage of the ageing

process, long time process, is the precipitation of carbides at dislocation regions. At this work the loading-unloading cycle tests are performed at room temperature and long time is required for the diffusion of the carbon atoms towards the dislocations lines at this temperature. Thus, the short time Snoek rearrangement process is supposed the main mechanism responsible for the increase of the upper yield limit during reloading.

In order to prove that the increasing of the upper yield point phenomenon is related with the iteration between carbon atoms and the dislocations, Snoek phenomenon, the loading-unloading cycle tests have been repeated with a DC04 mild steel. The carbon content of this mild steel is much lower than that of the TRIP 700. Therefore, the increase of the upper yield limit in the mild steel has to be lower than the one of the TRIP 700 and therefore a lower upper yield limit effect should be observed for this material.

In Table 2 the chemical composition of the tested mild steel, obtained by optical emission spectroscopy, is shown. In Fig. 10 the increase in the upper yield limit of both TRIP 700 steel and mild steel are shown (Fig. 10(b) and Fig. 10(a)). The hypothesis that the upper yield point is due to the Snoek short time rearrangement process is confirmed.

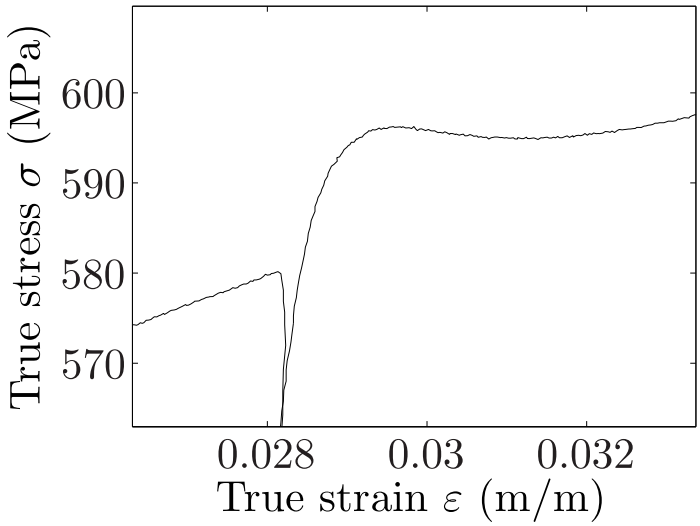

(a) Increase in the upper yield limit in the TRIP steel.

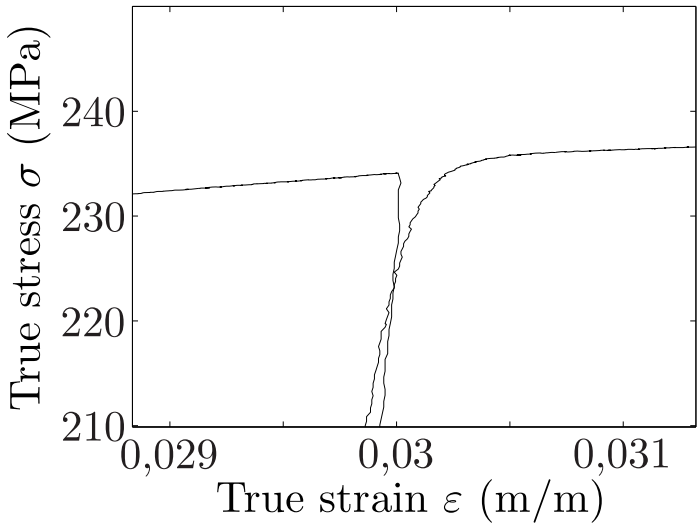

(b) Increase in the upper yield limit in the mild steel.

Figure 10: Snoek phenomenon comparative: a) the increase in the upper yield limit for the TRIP 700 and b) the increment in the upper yield limit for the DC04 mild steel.

5. General conclusions

The elastic behaviour of the TRIP 700 steel has been analysed using conventional tensile tests and loading-unloading cyclic tests. From the experimental results the following general conclusions have been obtained:

- Both conventional tensile tests and loading-unloading cyclic tests exhibit a similar hardening behaviour. Therefore, global hardening is not affected by the cycles
- The elastic modulus during loading as well as the chord modulus during unloading decrease as the pre-strain increases. This diminution in modulus is about 15-20% at 12% of pre-strain
- The non-linearity of the unloading phases can be explained by the dislocation bending phenomenon, whereas the unloading non-linearity is governed by different mechanisms being the microplastic strains the main one
- The reduction of the unloading elastic modulus is related to both phase transformation and dislocation rearrangement, but the latter is the main reason of the elastic modulus decrease
- The increment of the upper yield point shown in the loading phases could be explained by the Snoek short time rearrangement process

The understanding of the elastic modulus evolution of AHSS with the plastic strain and the experimental data shown in this article are a valuable source of the future reliable springback numerical models of industrial processes.

6. Acknowledgments

The work presented in this paper has been carried out with the financial support of the Department of Education, Universities and Research of the Basque Government as well as in cooperation with FAGOR ARRASATE Scoop and with the financial support of the INNPACTO National Programme (Spanish Science and Innovation Minister) for Public-Private Cooperation Project AVANROLL: Development of novel techniques and facilities for the manufacturing of high added value automotive compoenents (Project number IPT-020000-2010-020) and in cooperation with FAGOR ARRASATE Scoop and ORTIC AB within the frame of the EUROSTARS Project FUTROLL: Development of accurate 3D roll forming technology and machine to manufacture profiles for the automotive industry (Project number CIIP-20122007) and with the financial support of the Spanish agency CDTI, Centro para el Desarrollo Tecnológico Industrial.

References

Cleveland, R., Ghosh, A., 2002. Inelastic effects on springback in metals. International Journal of Plasticity 18, 769 –85.

Doege, E., Kulp, S., Sunderkotter, C., 2002. Properties and application of TRIP-steel in sheet metal forming. Steel Research 73, 303 –8.

Eggertsen, P.A., Mattiasson, K., 2011. On the identification of kinematic hardening material parameters for accurate springback predictions. International Journal of Material Forming 4, 103 –20.

Farías, D., 2006. Bake Hardening Response of DP800 and the Influence on the 'In Service Performance'. Master's thesis. Technische Universiteit Eindhoven.

Fei, D., Hodgson, P., 2006. Experimental and numerical studies of springback in air v-bending process for cold rolled TRIP steels. Nuclear Engineering and Design 236, 1847 –51.

Foreman, A.J.E., 1967. The bowing of a dislocation segment. Philosophical Magazine 15, 1011 –21.

Gelin, J., Thibaud, S., Boudeau, N., 2005. Modelling and simulation of the influence of forming processes on the structural behavior of high strength steels, USA. pp. 101 – 6.

Mendiguren, J., Cortés, F., Galdos, L., Berveiller, S., 2012. Strain path's influence on the elastic behaviour of the trip 700 steel. Materials Science & Engineering A .

Mendiguren, J., Trujillo, J.J., Cortés, F., Galdos, L., 2013. An extended elastic law to represent non-linear elastic behaviour: Application in computational metal forming. International Journal of Mechanical Sciences 77, 57 – 64.

Morestin, F., Boivin, M., 1996. On the necessity of taking into account the variation in the Young modulus with plastic strain in elastic-plastic software. Nuclear Engineering and Design 162, 107 – 16.

Perez, R., Benito, J., Prado, J., 2005. Study of the inelastic response of TRIP steels after plastic deformation. ISIJ International 45, 1925 –33.

Sun, L., Wagoner, R., 2011. Complex unloading behavior: Nature of the deformation and its consistent constitutive representation. International Journal of Plasticity 27, 1126 –44.

Thibaud, S., Boudeau, N., Gelin, J., 2002. Influence of initial and induced hardening in sheet metal forming. Int. J. Damage Mech 13, 107 –22.

Yu, H.Y., 2009. Variation of elastic modulus during plastic deformation and its influence on springback. Materials and Design 30, 846 – 50.